JACS
JOURNAL OF THE AMERICAN CHEMICAL SOCIETY
Communication
pubs.acs.org/JACS

High Thermoelectric Properties of n-Type $AgBiSe_2$

Lin Pan,* David Bérardan,* and Nita Dragoe

[†]Institut de Chimie Moléculaire et des Matériaux d'Orsay, Université Paris-Sud, UMR 8182, Orsay F-91405, France, and CNRS, Orsay F-91405, France

Supporting Information

ABSTRACT: We report on the thermoelectric (TE) performance of intrinsic n-type $AgBiSe_2$, a Pb-free material with more earth-abundant and cheaper elements than intrinsic p-type homologous $AgSbTe_2$. Pb doping changes n-type $AgBiSe_2$ to p-type but leads to poor electrical transport properties. Nb doping enhances the TE properties of n-type $AgBiSe_2$ by increasing the carrier concentration. As a result of the intrinsically low thermal conductivity (0.7 W m^{-1} K^{-1}), low electrical resistivity (5.2 mΩ cm), and high absolute Seebeck coefficient (−218 μV/K), the TE figure of merit (ZT) at 773 K is significantly increased from 0.5 for solid-state-synthesized pristine $AgBiSe_2$ to 1 for $Ag_{0.96}Nb_{0.04}BiSe_2$, which makes it a promising n-type candidate for medium-temperature TE applications.

The thermoelectric (TE) effect enables direct conversion of thermal energy to electrical energy and provides an alternative route for power generation and refrigeration.[1] The TE conversion efficiency of TE materials is an increasing function of the dimensionless figure of merit $ZT = S^2T/\rho\lambda$, where S, ρ, λ, and T are the Seebeck coefficient, electrical resistivity, thermal conductivity, and absolute temperature, respectively. Generally, the most successful route for enhancing ZT is reducing λ, particularly through nanostructuring.[2] Hence, many researchers have focused their attention on designing nanostructures or embedding nanoscale precipitates in bulk materials to limit the lattice thermal conductivity (λ_L) by scattering of long-wavelength phonons.[3−5] However, such materials with reduced dimensions are not easy to prepare and control. Besides, nanostructures may grow or dissolve during prolonged high-temperature operation.[6] Therefore, Pb-free bulk materials such as I−V−VI_2 compounds with intrinsically low λ_L have attracted much attention.[6] The ternary chalcogenide $AgSbTe_2$, as a typical example of a I−V−VI_2 compound, is well-known as a promising bulk p-type TE material for T = 500−800 K, mainly because of its low λ and high S.[7,8] $AgSbTe_2$ alloys with GeTe (so-called TAGS) with a maximum ZT value (ZT_{max}) of 1.5 at 750 K were considered the best TE materials for quite a long time.[9,10] $AgSbTe_2$ alloys with PbTe (so-called LAST) feature ZT_{max} = 2.2 at 800 K, which is the highest reported figure of merit for bulk TE materials at present.[11] However, the application of those alloys seems to be limited because of their thermodynamic instability and inhomogeneity, which make the alloys lose their excellent TE properties during long-term annealing at high temperatures.[8] In addition, all of these materials contain a significant amount of Te, which is scarce in the earth's crust. To allow for widespread use of TE materials in a variety of applications, inexpensive alternatives are needed. Therefore, $AgBiSe_2$ has attracted our interest as a homologue of $AgSbTe_2$ containing more earth-abundant elements. Previous studies reported that $AgBiSe_2$, with an intrinsically very low λ_L,[6] exhibits p-type semiconducting behavior when synthesized by a solution route, with ZT_{max} reaching 1.5 at 700 K.[12,13] Here we report that solid-state-synthesized pristine $AgBiSe_2$ is an intrinsic n-type semiconductor that can be switched to p-type by Pb doping. Moreover, with proper Nb doping, ZT of n-type $AgBiSe_2$ can reach 1 at 773 K at the optimum carrier concentration.

Experimental details can be found in the Supporting Information (SI). All of the compositions discussed in the text are nominal ones. Powder X-ray diffraction (PXRD) patterns for pristine $AgBiSe_2$ at room temperature (RT), 523 K, and 723 K are shown in Figure 1.

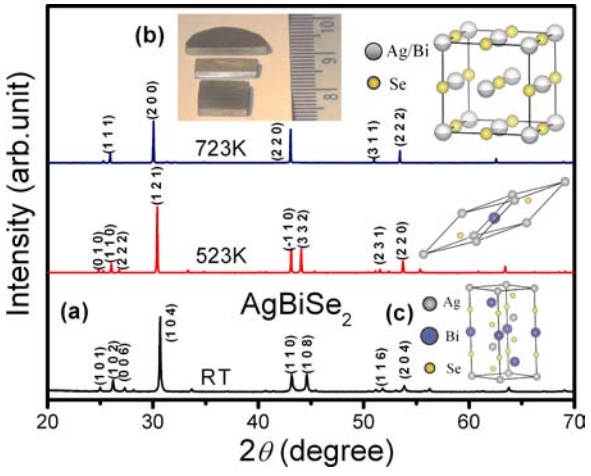

Figure 1. (a) PXRD patterns of pristine $AgBiSe_2$ at RT, 523 K, and 723 K. (b) Typical spark plasma sintering disk-shaped pellet and samples used in this study. (c) Crystal structures of hexagonal, rhombohedral, and cubic $AgBiSe_2$ at RT, 523 K, and 723 K, respectively.

$AgBiSe_2$ crystallizes in a hexagonal phase (space group $Pm\bar{3}1$) with a = 4.194 Å, c = 19.65 Å, and V = 300.9 $Å^3$ (100.3 $Å^3$ per formula unit) at RT; a rhombohedral phase (space group $R\bar{3}m$) with a = 4.184 Å and c = 19.87 Å in hexagonal settings and V = 301.3 $Å^3$ (100.4 $Å^3$ per formula unit) at 523 K; and a cubic phase (space group $Fm\bar{3}m$) with a = 5.930 Å and V = 208.5 $Å^3$ (104.25 $Å^3$ per formula unit) at 723 K. These results are in agreement

Received: December 21, 2012
Published: March 19, 2013

   dx.doi.org/10.1021/ja312474n | J. Am. Chem. Soc. 2013, 135, 4914−4917

with previously reported structural phase transitions of $AgBiSe_2$ from a low-temperature hexagonal α phase to a rhombohedral β phase at an intermediate temperature and then to a cubic γ phase at high temperature.[14] The volume change (ΔV) in going from the α to the β phase is very small. Indeed, this transition does not correspond to an important atomic rearrangement but more or less to an elongation of the unit cell in the [001] direction of the hexagonal lattice coupled with slight atomic displacements. However, ΔV is larger for the $\beta \rightarrow \gamma$ phase transition, and the thermal expansion coefficient in the cubic phase was estimated to be 57×10^{-6} from the temperature dependence of a (Figure S2 in the SI), which could be detrimental for TE applications. From our differential scanning calorimetry measurements (Figure S4a,b), the temperatures corresponding to the phase transitions are ~470 K ($\alpha \rightarrow \beta$) and ~570 K ($\beta \rightarrow \gamma$). Although $T_{\alpha\beta}$ is different from the previously reported literature value, it corresponds very well to the features observed in the transport property measurements (see below). This discrepancy can probably be explained by the very small heat flow associated with the $\alpha \rightarrow \beta$ transition, which makes it hard to detect by thermal analysis (Figure S4a,b).

The PXRD patterns for doped samples at RT (Figure 2a) show that the main diffraction peaks for $AgBi_{1-x}Pb_xSe_2$ and

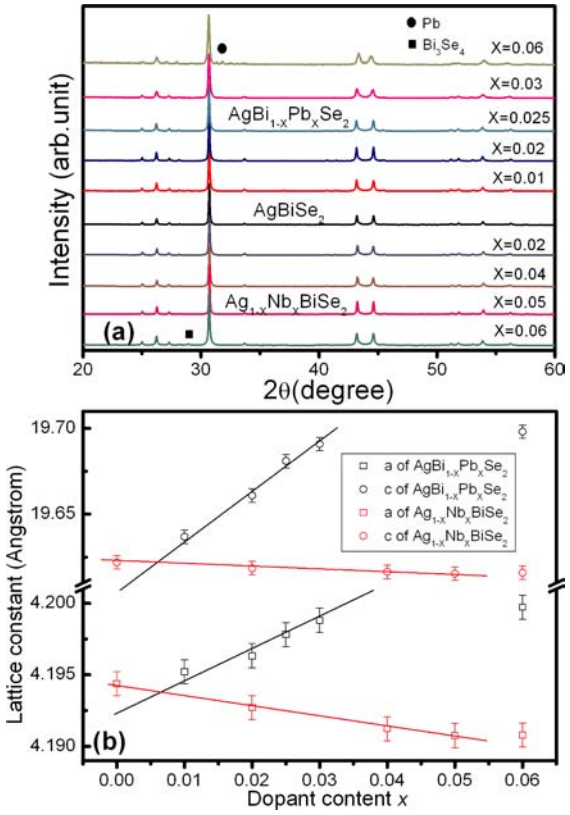

Figure 2. (a) PXRD patterns and (b) lattice constants of Pb-doped $AgBi_{1-x}Pb_xSe_2$ and Nb-doped $Ag_{1-x}Nb_xBiSe_2$ at RT. Solid lines in (b) are guides for the eyes.

$Ag_{1-x}Nb_xBiSe_2$ correspond to the low-temperature hexagonal phase of $AgBiSe_2$ (JCPDS no. 29-1441), with no other phases being detected in the XRD patterns except for the $x = 0.06$ samples. The accurate lattice parameters calculated from the PXRD data using Rietveld refinement (Figure 2b) indicate that a and c slightly increase (decrease) monotonically with increasing Pb (Nb) content. Indeed, the ionic radius of Pb (Nb) is larger (smaller) than that of Bi (Ag), which results in lattice expansion (shrinkage) with increasing Pb (Nb) content. The present results show that both Pb and Nb can be successfully introduced into $AgBiSe_2$, leading to the formation of $AgBi_{1-x}Pb_xSe_2$ and $Ag_{1-x}Nb_xBiSe_2$ series with solubility limits close to 0.04 and 0.05, respectively. Energy-dispersive X-ray analysis elemental mapping of $Ag_{0.97}Nb_{0.03}BiSe_2$ (Figure S1) evidenced a homogeneous distribution of Nb within the matrix, except for a minor amount of Nb inclusions (not detected in the PXRD patterns). Moreover, the obtained composition is in good agreement with the nominal composition. Low-magnification scanning electron microscopy images of the fracture surfaces of typical samples (Figure S3) indicated that the obtained samples were homogeneous with low porosity.

The temperature dependences of the electrical conductivity ρ and the Seebeck coefficient S for $AgBi_{1-x}Pb_xSe_2$ (x = 0.01, 0.02, 0.025, 0.03, 0.06) over the range 50−300 K are shown in Figure 3. We observed a negative value of S with semiconductor-like

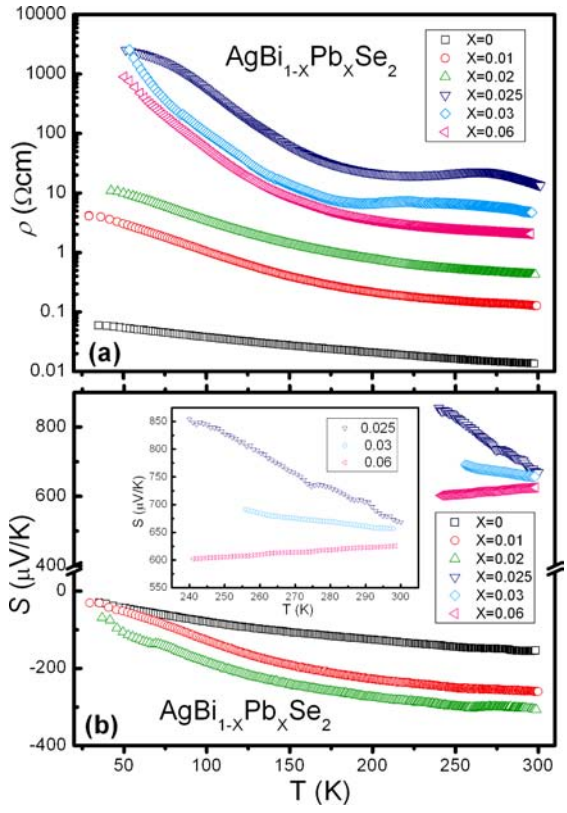

Figure 3. Temperature dependences of (a) ρ and (b) S for $AgBi_{1-x}Pb_xSe_2$ from 20 to 300 K. Inset of (b): enlargement of the S plot for $AgBi_{1-x}Pb_xSe_2$ (x = 0.025, 0.03, and 0.06) from 240 to 300 K.

behavior, which indicates that pristine $AgBiSe_2$ obtained by solid-state synthesis is an n-type semiconductor. This result is different from the one reported for solution-synthesized $AgBiSe_2$, which exhibits p-type conductivity.[12,13] This difference may originate either from contamination during the solution synthesis or from a slightly different stoichiometry of the compound that could result in unintentional doping, including for example Ag vacancies.[13] However, as the previous reports did not mention any carrier concentration measurements, it is hard to give a definitive explanation of this discrepancy. The values of ρ and S for pristine $AgBiSe_2$ at RT are 13.8 mΩ cm and −154 μV/K, respectively. One can see that as the Pb content (x) increases

dx.doi.org/10.1021/ja312474n | J. Am. Chem. Soc. 2013, 135, 4914−4917

from 0 to 0.02, ρ and |S| for $AgBi_{1-x}Pb_xSe_2$ increase monotonically. The negative sign of S for $AgBi_{1-x}Pb_xSe_2$ (x = 0, 0.01, 0.02) means that electrons are still the major charge carriers in these samples. However, when x increases from 0.02 to 0.025, the sign of S abruptly changes from negative (−307 μV/K at RT) to positive (670 μV/K at RT). Meanwhile, ρ increases from 0.43 to 13.6 Ω cm at RT. This result indicates that the major charge carriers of $AgBi_{1-x}Pb_xSe_2$ are holes rather than electrons at higher Pb content, with the crossover lying somewhere between x = 0.02 and 0.025. This switch in the type of major carrier was confirmed by Hall effect measurements, which showed a positive slope of the Hall resistivity versus magnetic field for the x = 0.03 sample. However, because of the large ρ, the measurement was very noisy, and we can give only a rough estimate of the hole concentration, which is on the order of 10^{18} cm^{-3}. We note that a small amount of hole doping is sufficient to switch this material from n-type to p-type, which could explain the different behavior observed for solution-synthesized samples. With a further increase in x to 0.06, ρ and S for $AgBi_{1-x}Pb_xSe_2$ decrease to 2.1 Ω cm and 626 μV/K at RT. This behavior can be easily explained by a simple electron count. Starting from n-type pristine $AgBiSe_2$, Pb^{2+} doping at Bi^{3+} sites first results in a decrease in the electron concentration and thus to an increase in both ρ and |S|. When the Pb^{2+} concentration exceeds the intrinsic electron concentration, the compounds switch to p-type. Last, further increases in the Pb^{2+} concentration lead to increases in the hole concentration and thus to a decrease of ρ and |S|. The present work indicates that Pb doping can tune intrinsically n-type $AgBiSe_2$ to p-type, although this results in poor electrical transport performance, which is of small interest for TE applications. However, this tunable transition from n-type to p-type with doping could be useful for electronic applications, for example, with easily processable p−n junctions.

The temperature dependences of ρ and S for $Ag_{1-x}Nb_xBiSe_2$ (x = 0, 0.02, 0.04) over the range 20−773 K are shown in Figures 4 and S5. The negative value of S for $Ag_{1-x}Nb_xBiSe_2$ combined with semiconductor-like behavior indicates that for all x, $Ag_{1-x}Nb_xBiSe_2$ is an n-type semiconductor at temperatures below ∼470 K, where the $\alpha \rightarrow \beta$ phase transition takes place. In the β phase, metallic-like behavior of ρ is observed up to the $\beta \rightarrow \gamma$ phase transition at ∼570 K, after which ρ decreases again. The value of |S| for $Ag_{1-x}Nb_xBiSe_2$ increases with increasing temperature from 20 to ∼470 K in the α phase, then increases quickly from ∼470 K to ∼570 K in the β phase, and finally continues to increase after the $\beta \rightarrow \gamma$ phase transition. Similar anomalies of S have been reported in p-type solution-synthesized $AgBiSe_2$, with reversible p−n−p switching of the sign of S when going from the hexagonal to the rhombohedral to the cubic phase.[13] In our n-type material, we did not observe any change in the sign with temperature, but S became "more n-type" between the two phase transitions. In $Ag_{10}Te_4Br_3$, a similar p−n−p switching behavior has been attributed to a charge density wave (CDW) linked to a Peierls transition[15] that influences the electronic density of states close to the Fermi level, and it has been suggested that this thermopower modulation could be used to develop improved TE materials.[16] A strong anomaly was also observed in the temperature dependence of the thermal diffusivity (Figure S7).

In regard to the Nb fraction (x) dependence of the transport properties, ρ and |S| for $Ag_{1-x}Nb_xBiSe_2$ both decrease monotonically with increasing x for the entire investigated temperature domain. For instance, at RT, ρ and |S| decrease from 13.8 mΩ cm and 154 μV/K for pristine $AgBiSe_2$ to 4.3 mΩ cm and 85 μV/K for $Ag_{0.96}Nb_{0.04}BiSe_2$, respectively. When x is increased to 0.05, ρ and |S| keep decreasing, which leads to a decrease in the TE power factor S^2/ρ (Figure S5). The carrier concentrations for $Ag_{1-x}Nb_xBiSe_2$ from 20 to 300 K were calculated using the measured Hall coefficients (Figure S3 and S4). The electron concentration increases with increasing temperature, which further confirms that $Ag_{1-x}Nb_xBiSe_2$ is an n-type semiconductor in the low-T hexagonal phase. With increasing x, the electron concentration of $Ag_{1-x}Nb_xBiSe_2$ increases monotonically (e.g., from 1.5×10^{19} cm^{-3} for pristine $AgBiSe_2$ to 6.5×10^{19} cm^{-3} for $Ag_{0.96}Nb_{0.04}BiSe_2$ at RT). This result is consistent with electron doping upon the introduction of Nb into the unit cell. Moreover, this result indicates that the decreases in ρ and |S| with increasing x for $Ag_{1-x}Nb_xBiSe_2$ mainly originate from the increasing electron concentration and decreasing carrier mobility (Figure S6). It is noteworthy that the resistivity anomaly is strongly reduced by Nb substitution, which disturbs the formation of the CDW, probably as a result of the disorder induced in the Ag−Bi sublattice when Ag is substituted with Nb. This shows that the thermopower modulation, and therefore the TE performance, could be controlled by fine-tuning of the cationic substitution.

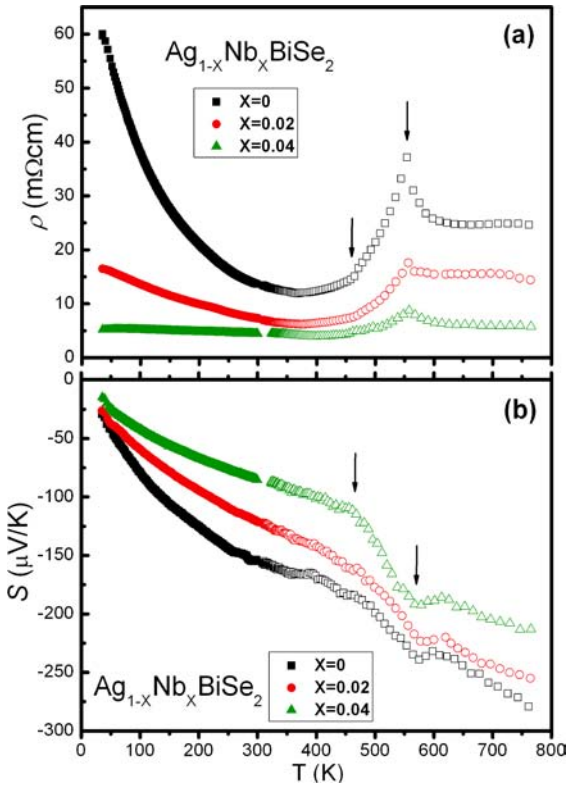

Figure 4. Temperature dependences of (a) ρ and (b) S for $Ag_{1-x}Nb_xBiSe_2$ from 20 to 773 K (solid markers, low-T measurement system; open markers, high-T measurement system).

The temperature dependence of the thermal conductivity λ for $Ag_{1-x}Nb_xBiSe_2$ (x = 0, 0.02, 0.04) is plotted in Figure 5a. At RT, λ for pristine $AgBiSe_2$ is 0.64 W m^{-1} K^{-1}, and it remains nearly constant as T increases to ∼470 K, in agreement with the previous report of Morelli et al.[6] However, λ for pristine $AgBiSe_2$ decreases as T increases from ∼470 K (at the $\alpha \rightarrow \beta$ phase transition) up to ∼570 K, where the $\beta \rightarrow \gamma$ phase transition occurs. Above ∼570 K, λ increases with increasing T. It is well-known that anharmonicity of the chemical bonds drives the phonon−phonon umklapp and normal processes that intrinsically limit the high-T value of λ_L.[17] The anharmonicity of $AgBiSe_2$

dx.doi.org/10.1021/ja312474n | J. Am. Chem. Soc. 2013, 135, 4914−4917

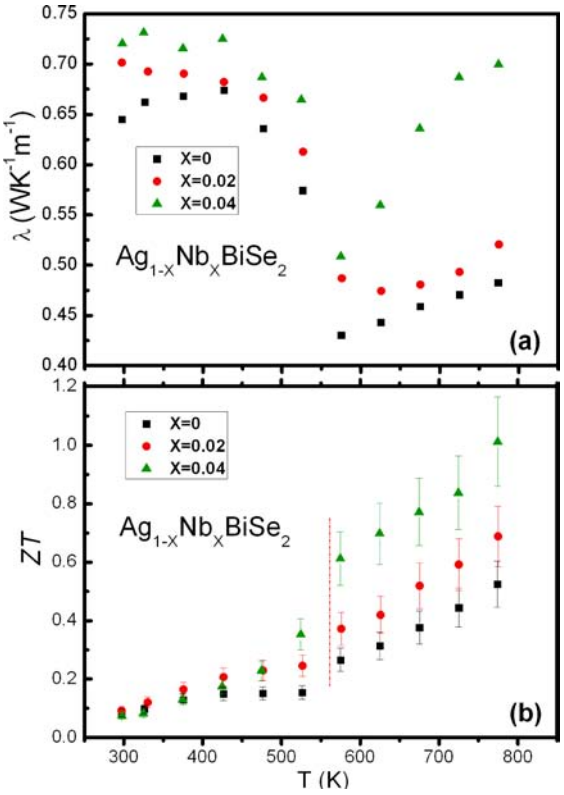

Figure 5. Temperature dependences of (a) λ and (b) ZT for $Ag_{1-x}Nb_xBiSe_2$ from 300 to 773 K. The dashed line in (b) is a guide for the eyes to distinguish the γ phase from the β phase.

is even higher than that of PbTe, probably because of the presence of Bi, resulting in a phonon−phonon-limited value of λ_L smaller than that of PbTe.[6,18] For a solid, λ is the sum of λ_L and the carrier thermal conductivity (λ_C), which can be estimated using the Wiedemann−Franz law. λ_C was estimated to be less than 9% of λ for pristine $AgBiSe_2$ at RT and ∼16% at 773 K. These results indicate that λ for pristine $AgBiSe_2$ is mainly determined by phonon transport. Moreover, λ_L decreases with increasing Nb content, which may originate principally from increasing phonon scattering as the dopant and carrier concentrations are increased (Figure S7). However, λ for $Ag_{1-x}Nb_xBiSe_2$ increases with increasing x because of the increase in the electronic contribution.

The figure of merit ZT resulting from the combination of the electrical and thermal transport properties over the range 300−773 K is shown in Figure 5b. Here, S, ρ, and λ should be measured in the same direction of the pellet. In our present experiment, S and ρ were measured in a direction perpendicular to the pressing direction, while λ was determined in a direction parallel to the pressing direction. However, values of λ in different directions determined at high temperature in the cubic phase of $Ag_{1-x}Nb_xBiSe_2$ are identical, as the transport properties are isotropic; moreover we checked one of the Nb-doped samples and found that the transport properties were indeed identical in both directions within the uncertainty of the measurements (Figure S9). ZT increases with temperature, with ZT_{max} at 773 K equal to 0.5 for pristine $AgBiSe_2$ and 1 for $Ag_{0.96}Nb_{0.04}BiSe_2$. Therefore, our results indicate that the TE properties of $AgBiSe_2$ can be remarkably improved by increasing the carrier concentration through Nb doping. We note that this large ZT was obtained for a bulk system and that further improvements could be made by using other dopants or by nanostructuration.

In summary, the carrier type in $AgBiSe_2$ can be tuned from intrinsic n-type to p-type by Pb doping. The thermoelectric properties of n-type $AgBiSe_2$ are enhanced by Nb doping because of the increased carrier concentration. Low electrical resistivity, low thermal conductivity, and high absolute values of the Seebeck coefficient were achieved, resulting in a high ZT of 1 at 773 K for $Ag_{0.96}Nb_{0.04}BiSe_2$, which makes it a promising candidate for medium-temperature n-type TE applications.

■ ASSOCIATED CONTENT

Supporting Information

Experimental details and additional data. This material is available free of charge via the Internet at http://pubs.acs.org.

■ AUTHOR INFORMATION

Corresponding Author

greenspan513@163.com; david.berardan@u-psud.fr

Notes

The authors declare no competing financial interest.

■ ACKNOWLEDGMENTS

This work was supported by the ANR through the project OTHer (ANR 2011 JS08 012 01).

■ REFERENCES

(1) DiSalvo, F. J. *Science* **1999**, *285*, 703.
(2) Dresselhaus, M. S.; Chen, G.; Tang, M. Y.; Yang, R.; Lee, H.; Wang, D.; Ren, Z.; Fleurial, J. P.; Gogna, P. *Adv. Mater.* **2007**, *19*, 1043.
(3) Zhao, L. D.; He, J. Q.; Hao, S. Q.; Wu, C. I.; Hogan, T. P.; Wolverton, C.; Dravid, V. P.; Kanatzidis, M. G. *J. Am. Chem. Soc.* **2012**, *134*, 16327.
(4) Mehta, R. J.; Zhang, Y. L.; Karthik, C.; Singh, B.; Siegel, R. W.; Borca-Tasciuc, T.; Ramanath, G. *Nat. Mater.* **2012**, *11*, 233.
(5) He, J. Q.; Girard, S. N.; Zheng, J. C.; Zhao, L. D.; Kanatzidis, M. G.; Dravid, V. P. *Adv. Mater.* **2012**, *24*, 4440.
(6) Morelli, D. T.; Jovovic, V.; Heremans, J. P. *Phys. Rev. Lett.* **2008**, *101*, No. 035901.
(7) Du, B. L.; Li, H.; Xu, J. J.; Tang, X. F.; Uher, C. *Chem. Mater.* **2010**, *22*, 5521.
(8) Wojciechowski, K. T.; Schmidt, M. *Phys. Rev. B* **2009**, *79*, No. 184202.
(9) Cook, B. A.; Kramer, M. J.; Wei, X.; Harringa, J. L.; Levin, E. M. *J. Appl. Phys.* **2007**, *101*, No. 053715.
(10) Yang, S. H.; Zhu, T. J.; Sun, T.; He, J.; Zhang, S. N.; Zhao, X. B. *Nanotechnology* **2008**, *19*, No. 245707.
(11) Hsu, K. F.; Loo, S.; Guo, F.; Chen, W.; Dyck, J. S.; Uher, C.; Hogan, T.; Polychroniadis, E. K.; Kanatzidis, M. G. *Science* **2004**, *303*, 818.
(12) Xiao, C.; Xu, J.; Cao, B. X.; Li, K.; Kong, M. G.; Xie, Y. *J. Am. Chem. Soc.* **2012**, *134*, 7971.
(13) Xiao, C.; Qin, X. M.; Zhang, J.; An, R.; Xu, J.; Li, K.; Cao, B. X.; Yang, J. L.; Ye, B. J.; Xie, Y. *J. Am. Chem. Soc.* **2012**, *134*, 18460.
(14) Manolikas, C.; Spyridelis, J. *Mater. Res. Bull.* **1977**, *12*, 907.
(15) Nilges, T.; Lange, S.; Bawohl, M.; Deckwart, J. M.; Janssen, M.; Wiemhöfer, H.-D.; Decourt, R.; Chevalier, B.; Vannahme, J.; Eckert, H.; Weihrich, R. *Nat. Mater.* **2009**, *8*, 101.
(16) Osters, O.; Bawohl, M.; Bobet, J.-L.; Chevalier, B.; Decourt, R.; Nilges, T. *Solid State Sci.* **2011**, *13*, 944.
(17) Ioffe, A. F. *Physics of Semiconductors*; Infosearch: London, 1958.
(18) Nielsen, M. D.; Ozolins, V.; Heremans, J. P. *Energy Environ. Sci.* **2013**, *6*, 570.